Integrating Core Data and Wireline Data for Formation Evaluation and Characterization of Shale Gas Reservoirs*

John Quirein[1], Dan Buller[2], Jim Witkowsky[1], and Jerome Truax[1]

Search and Discovery Article #41073 (2012)*
Posted November 19, 2012

*Adapted from extended abstract prepared in conjunction with oral presentation at AAPG International Convention and Exhibition, Singapore, 16-19 September 2012, AAPG©2012

[1]Halliburton, Houston, TX (john.quirein@halliburton.com)
[2]Halliburton, Shreveport, LA

Abstract

The development and production of shale gas reservoirs involves the drilling, interpretation, and stimulation of many vertical and horizontal wells, all with varying amounts of core and wireline data. This paper presents several Haynesville shale interpretation workflows for scenarios with varying combinations of core and wireline/LWD data, and emphasizes answers obtained from wireline/LWD data. It demonstrates how wireline and core data can be combined to provide total organic carbon (TOC), total porosity, gas filled porosity, mineralogy, grain density, and mechanical properties, including anisotropy and an indicator of where to fracture.

Generally, TOC is measured in weight percent, and is associated with the organic compound, kerogen. The TOC of 10 wt% is associated with an approximate kerogen volume of 20 vol%. Unfortunately, the neutron and density logs sense kerogen as an additional porosity. Consequently, with an actual kerogen volume of 20 vol%, and without accounting for kerogen in the interpretation, the traditional neutron-density cross plot porosity will be high by 20 vol%. Any quantitative log interpretation predicting porosity and gas saturation must properly predict the amount of kerogen. This paper presents an approach for predicting kerogen volume through calibration to core data to enable an initial porosity prediction. A Haynesville example is used to show that, when geochemical logs and core XRD are available, mineralogy and grain density can be predicted from wireline logs, enabling a more accurate prediction of porosity gas saturation, and mineralogy based shale brittleness index.

Economic recovery of gas from shale reservoirs requires optimal multistage hydraulic stimulation in horizontal wells. This type of formation evaluation requires careful correlation and calibration to petrophysical measurements and interpretations obtained in either vertical pilot holes or direct offset wells. An example of a horizontal well using LWD sonic and pulsed neutron cased hole data is presented. Fracture stages for the logged horizontal well were evaluated vs. the log data. Generally, lower normalized treating pressures per fracture stage are noted where lower clay volumes exhibit less transverse anisotropy and a higher calculated shale brittleness index. Radioactive tracer and production log data also confirm lower amounts of gas production from zones that are apparently fractured, but are more ductile and clay-rich.

Introduction

The Haynesville shale is a black, organic-rich shale that covers Caddo, Bossier, De Soto, Red River, and Bienville Parishes in North Louisiana and mainly Harrison, Panola, Shelby, and San Augustine Counties in East Texas The depth ranges from about 10,300 ft in the northwest part of the play to about 14,000 ft in the southeast. The Bossier shale lies above the play and the Haynesville lime or Smackover lime lie below it throughout the area. Both of these formations can be drilling targets, but the Haynesville Shale is of special interest because of generally thicker net pay and higher reservoir pressure, with a gradient between 0.85 and 0.9 psi/ft. Varying depositional environments have left the shale with thickness varying between 80 and 350 ft and facies varying between calcite-rich shale with little clay to silica-rich shale with large amounts of bedded clay and lesser amounts of calcite (Parker et al. 2009).

The development and production of shale gas reservoirs involve drilling, interpretation, and stimulation of many vertical and horizontal wells, all with varying amounts of core and wireline data. This paper presents several Haynesville shale interpretation workflows for scenarios with varying combinations of core and wireline/LWD data and emphasizes answers obtained from wireline/LWD data. It demonstrates how wireline and core data can be combined to provide total organic carbon (TOC), total porosity, gas-filled porosity, mineralogy, grain density, and mechanical properties, including anisotropy and an indicator of where to fracture.

Generally, TOC is measured in weight percent (wt%) and is associated with the organic compound, kerogen. The TOC of 10 wt% is associated with an approximate kerogen volume of 20%. Unfortunately, the neutron and density logs sense kerogen as an additional porosity. Consequently, with an actual kerogen volume of 20% and without accounting for kerogen in the interpretation, the traditional neutron-density cross-plot porosity will be high by 20%. Any quantitative log interpretation predicting porosity and gas saturation must properly predict the amount of kerogen. This paper presents an approach for predicting kerogen volume through calibration of core data to enable an initial porosity prediction. A Haynesville example is used to show that, when geochemical logs and core XRD are available, mineralogy and grain density can be predicted from wireline logs, enabling a more accurate prediction of porosity, gas saturation, and a mineralogy-based shale brittleness index.

Economic recovery of gas from shale reservoirs requires optimal multistage hydraulic stimulation in horizontal wells. This type of formation evaluation requires careful correlation and calibration to petrophysical measurements and interpretations obtained in either vertical pilot holes or direct offset wells. An example of a horizontal well using LWD sonic and pulsed-neutron cased-hole data is presented. Fracture stages for the logged horizontal well were evaluated vs. the log data. Generally, lower normalized treating pressures per fracture stage are noted where lower clay volumes exhibit less transverse anisotropy and a higher calculated shale brittleness index. Radioactive tracer and production log data also confirm lower amounts of gas production from zones that are apparently fractured but are more ductile and clay-rich. Figure 1 summarizes the workflow discussed above.

Predicting Total Organic Carbon (TOC)

As discussed in the introduction, to determine an accurate porosity, it is imperative to determine the amount of TOC/kerogen, as kerogen is seen as additional porosity by the neutron/density logs. Passey (1990) and many others have developed techniques for predicting core TOC wt% from log data. We propose maintaining this historical approach and attempt to predict TOC wt% from log data independent of the final volumetric analysis, which will attempt to predict the mineralogy, porosity, and gas-free porosity. Three potential ways of computing TOC from log data considered here are: a) directly by regression of core TOC versus core bulk density; b) directly by regression of core TOC versus core or wireline Uranium; and c) applying the Δ log R techniques, Passey (1990). Our general observations have shown that TOC from bulk-density regression is the superior method; although, in bad hole, the sonic-resistivity Δ log R prediction is an attractive alternative, with the uranium log being used to help select the baseline (shale zone with no TOC) depth for calibration. As an example, predicting TOC from the bulk density will be presented for Haynesville shale, Panola County, Texas well, Quirein et al (2010). This method is particularly attractive, as both the bulk density and wt% TOC are available from core data at the same resolution. The simplicity and adequacy of the approach is shown in Figure 2, which compares in a cross-plot the core bulk density and core wt% TOC. This equation should be valid at least for the Haynesville within Panola County but could be expected to vary slightly in other counties as thermal maturity varies.

Recently, the concept of kerogen porosity has gained importance (Ramirez et al. 2011), as it implies a dual-porosity system, and the nature of this system should affect well production. Recent work by Curtis et al. (2011) using scanning transmission electron microscopy (STEM) suggests that kerogen porosity can exceed 14.4% in the Barnett shale and was estimated to be approximately 6% for a single Haynesville sample. Images of kerogen from the Barnett shale showed a sponge-like internal structure, whereas STEM images of the Haynesville shale showed significant and increased amounts of phyllosilicate porosity (at a smaller scale than SEM), with less global organization of clay platelets than local organization. Figure 3 shows the different types of shale porosity (Curtis et al. 2011). The lower, middle template illustrates how kerogen, kerogen porosity, and pyrite all occur concurrently. This association occurs for all the wells in our Haynesville database, as illustrated by Figure 4 and Figure 5.

Predicting Mineralogy, Porosity, and Gas-Filled Porosity

The proposed technique, similar to the method proposed by Herron et al. (2011), is a conventional, inverse approach that uses traditional nuclear, electrical, acoustic, and geochemical measurements, as well as models defined by tool-response equations, tool-response parameters, and interpretation-constraint equations. The geochemical measurements are necessary whenever the grain density is varying rapidly, which is the case as the Haynesville shale transitions into the Haynesville limestone, Quirein et al. 2012. In addition, a necessary component for a successful interpretation is the use of the proper parameters, which, in this case, are the mineral geochemical parameters and grain densities. This can all be accomplished within the context of the workflow proposed in Figure 6 and with representative results presented by Figure 7.

The results were obtained using neutron and density logs, geochemical logs, and shallow and deep resistivity logs to enable the water saturation to vary. TOC, estimated as discussed previously, was also input to the model. Figure 7 shows the results for a single Haynesville well. Track 1 presents the correlation logs, and Track 2 depicts the mineralogy, from left to right, kerogen, chlorite, illite, pyrite (red), sodium feldspar (orange), calcite, quartz, clay-bound water, free water, and gas-filled porosity. Track 3 presents the fluid volumes (gas, clay-

bound water, and free water), but also includes the kerogen matrix volume. The yellow circles represent the core gas-filled porosity, and the green circles show the core porosity. The volume of gas is broken down into its matrix (red) and kerogen (dull red) gas-filled porosity. Track 4 compares the core and well logs TOC. Track 5 presents the grain density, and Track 6 presents pyrite. Table 1 summarizes the correlation coefficient and root-mean squared error for the illustration well using core data. The well log interpretation agrees with the core data very well.

Figure 8 illustrates both the success and limitation of a constant matrix grain-density interpretation. Here, pyrite is from regression to TOC, and a remaining matrix grain density exclusive of TOC is assumed to be 2.71 g/cc. The geochemical and neutron logs are not used in the interpretation. In Figure 8, the blue curves are the results from using a full suite of logs, including the geochemical logs, and the red curves are the results excluding the geochemical logs (with the constant grain density assumption). The close comparison for much of the Haynesville formation suggests the assumption of a constant grain density, augmented by the amount of TOC and pyrite, to predict grain density is generally valid. However, an exception occurs in the region enclosed by the green rectangle where the grain density is changing rapidly, as illustrated by the core data in Track 5. This results in a 2-pu porosity error, which, in this case, equates to a 2-pu error in gas-filled porosity, as can be observed in Track 3.

Mechanical Properties, Sonic Logging, and Anisotropy

Sonic logs respond to (acoustic) anisotropy in various ways (Market et al., 2010). Compressional waves travel parallel to the wellbore and do not generally split, so we see one velocity that can be affected by the wellbore angle, meaning that if we measure the same formation at 0°, 30°, 60°, and 90°, we will observe different velocities (Hornby et al. 2003). In simple vertical wells, the compressional wave measures the vertical velocity of the formation (Figure 9a). In a high-angle well, the compressional wave measures a velocity that is between the vertical and horizontal velocities (Figure 9b), much as traditional resistivity tools would measure a resistivity value between Rh and Rv. Shear waves, however, propagate perpendicular to the axis of the tool and will polarize if the formation is anisotropic. In the case of shales, if the formation is composed of layers that are finer than the vertical resolution of the tool (which is on the order of 1.5 to 3 ft, depending on the tool and processing method) and the tool is perpendicular to the layers, the observed velocities will be an average of the multiple layers. In a horizontal well, the compressional waves travel parallel to the axis of the tool, which, in this case, means that they will measure the horizontal (x-axis) velocity. Shear waves travel perpendicular to the axis of the tool (in this case the y- and z- axis of the plane). Those waves travelling in the y-direction are travelling through one layer and, thus, have a simple route of propagation. The shear waves travelling in the z-direction, however, are travelling perpendicular to the layers. The layers will slow down the waves and make propagation more difficult.

In a transversely isotropic (TIV) medium with the z-axis the axis of symmetry, the elements of the stiffness tensor can be computed from the measured compressional, shear, and Stoneley-tube wave velocity (Fryman 2010 and Higgins et al. 2008). This is accomplished through correction for well deviation and implementation of the ANNE model (Schoenberg and Sayers 1996) and can be performed in vertical or horizontal wellbores. From the stiffness tensor, the vertical and horizontal Young's Modulus and Poisson's ratio can be computed, as shown by Higgins et al. (2008). It is mentioned that the ANNE model is an approximation and needs to be validated or refined for each shale

reservoir. The ANNE model assumes the Thompson anisotropy parameter δ is 0, and as a result, the following equation holds in a TIV medium and can be used to provide the vertical compressional velocity in a horizontal wellbore:

$$V^2_{compressional\_horizontal} = 2(V^2_{shear\_horizontal} - V^2_{shear\_vertical}) + V^2_{compressional\_vertical} \quad (1)$$

Laboratory testing shows that Young's Modulus is higher measured horizontally than it is vertically, while the Poisson's ratio is, on average, slightly lower measured horizontally than vertically. This significant transverse anisotropy observed in the Young's Modulus can be classified as (Buller 2010):

$$\Delta YME\_TIV = \frac{E_h - E_v}{E_v} \times 100 \quad (2)$$

The Δ*YME_TIV* term quantifies the percentage increase in the horizontal Young's Modulus over the vertical. A cross-plot, as shown in Figure 10, of this anisotropy term with differing minerals reveals that we can model this anisotropy as a linear function of clay volume. Large values of Δ*YME_TIV* imply ductile rock, whereas small values of Δ*YME_TIV* imply brittle rock. Thus, the Δ*YME_TIV* can be used to select lateral landing points from pilot holes. When sonic log data is not available, this can be compromised to zones with minimal clay.

This 'clay effect' serves to increase the minimum horizontal stress required for hydraulic-fracture initiation and subsequent treating pressures by increasing the term in the stress equation, as shown by Eq. 3.

$$\sigma_{H\,\min} \propto \frac{E_h}{E_v}\left(\frac{\nu_v}{1-\nu_h}\right) \quad (3)$$

This "clay effect," or lack of, can be seen in a horizontal well by direct viewing of the sonic well log data, as shown in Figure 11.

Horizontal Well Example

This horizontal well example is the BP, T.W. George A9H located in Harrison County, TX. A horizontal target consisting of the lower Haynesville shale "A" and upper Haynesville shale "B" was chosen for this well. Interpretation of a vertical offset well suggests that the Haynesville A and B shales are very homogeneous, having a constant 30% clay volume. A 4,300-ft lateral was drilled and correlated, as shown in Figure 12. The horizontal well was placed on target except for the two frac stages nearest the toe where angle was dropped. A complete horizontal evaluation was performed on this well, and all lessons and calibrations from the vertical wells were applied.

To simplify the analysis, we characterize anisotropy effects with the ratio of slow to fast shear travel times. A low TIV ratio (DTS slow/DTS fast) should equate to a higher brittleness index (Rickman et al. 2008). A higher TIV ratio should equate to a more ductile zone with a lower

brittleness index. Also computed is a “frac index,” which is the ratio of the brittleness index to the TIV ratio. Interpretation results are shown in Figure 13 below.

All logs indicate that we have varying amounts of clay between 25 and 40% The lower porosity zone located halfway down the lateral is shown to be partially dolomitized by the LIBS Chemostratigraphy data and is a suspected sequence boundary between the Haynesville “A” and the Haynesville ‘B” zones. Even with the clay volume, the effective porosity is still quite good at an average of 7%. The calculated brittleness index is clearly seen to be varying with the clay volume, and the fracture index is showing no obvious overly ductile intervals that would warrant staying away from. The TIV ratio is plotted next to the brittleness index, and a frac index is calculated using both as inputs. The bright green-coded frac index is highlighting the best opportunity for creating fracture conductivity along the horizontal well.

Without using any of the acquired horizontal well-evaluation data, the well was subsequently completed using 10 separate frac stages with perforations equally spaced every 110 ft along the horizontal well. Each stage had four sets of perforations with 12 shots per cluster. Each frac stage was designed as a generic water frac attempting to place 80,000 lbs of 100-mesh sand and 220,000 lbs of 40/80 hydro prop. All stages pumped to completion as designed on this well except for stage 5, which screened out early. Frac stage 5 was subsequently determined to be a mechanical problem at surface and not a downhole treatment issue. Horizontal production-log profiling confirms a disturbing finding that has long been suspected. On average, only two sets of perforations per frac stage are actually contributing any appreciable gas, which would lead one to suspect that there are sound mechanical reasons to perforate areas of highest brittleness and lower TIV anisotropy effects to achieve better post-frac fracture conductivity. Even though not all stage perforations are contributing, or some potentially not fractured, most of the proppant was placed in every stage on this well (except stage 5). There is good gas associated throughout the Haynesville “A”, “B”, and “C” zones. It is hypothesized that the relatively constant and lower clay volume below 40% contributed to better results on this well.

Conclusions

A workflow for shale gas reservoir evaluation in vertical wells has been presented. The initial step for the workflow is predicting TOC, which must be accurately accomplished so that subsequent accurate predictions of porosity and hydrocarbon can be obtained. There are correlations between, TOC, pyrite and sulfur, which must be addressed.

Prediction of mineralogy, porosity, and hydrocarbon can be complicated and is best accomplished using a complete set of logs and core data, including geochemical logs, XRD, and traditional core data obtained using the GRI crushed-sample approach. The preferred interpretation technique is a conventional inverse approach that uses traditional nuclear, electrical, acoustic, and geochemical measurements, as well as models defined by tool-response equations, tool-response parameters, and interpretation-constraint equations.

The geochemical measurements are necessary whenever the grain density is varying rapidly, which is the case as the Haynesville shale transitions into the Haynesville limestone. Mineral grain densities can be estimated from XRD and core grain-density data. Accurate mineral weight fractions and accurate mineral densities are necessary for predicting an accurate grain density.

As we have seen through the extensive petrophysical evaluations performed, shales are neither isotropic nor homogeneous, and extensive core analysis is necessary to build any comprehensive log models. In the case of the Haynesville shale in East Texas, total clay volume and clastic dilution of normally calcareous shale can cause large swings in relative brittleness and ductility that need to be accounted for in the horizontal wells. This is because horizontal completion efficiency is governed by both intrinsic heterogeneity (near wellbore) and extrinsic stresses (far field) acting on the formation.

Various solutions for obtaining best estimates of basic mechanical properties along the horizontal well have been demonstrated. Because of the horizontal anisotropy layering effects, a premium solution exists by coupling basic triple-combo data with a dipole sonic. This can be achieved by either LWD acquisition in open hole or wireline conveying a PNS Triple Combo surrogate and a X-Y Cross Dipole in cased hole. A standalone pulsed-neutron spectroscopy log is a very cost-effective solution as well, but it can only get at estimates of TIV anisotropy through its lithology estimates of total clay.

Whichever horizontal formation evaluation solution is chosen, the data acquired needs to be integrated into the completion design. The data clearly supports shooting less perforation clusters per frac stage, and the logs support where to optimally place those perforations. In this manner, depending on the lithology encountered, more frac stages can be placed along most long-reach laterals.

Lateral placement rules will dictate all well performance. You cannot frac from bad rock into good and expect that it will produce at high rates. Pre-drill vertical formation evaluation needs to be pursued with diligence and then optimum horizontal geosteering technology employed. Even if the wells are geosteered, they still need to be logged for picking optimum stimulation intervals.

Acknowledgements

The authors gratefully acknowledge the support of BP Exploration & Production, Houston for the use of their data and their contributions, and Halliburton Energy Services for their support.

References

Buller, D., S. Hughes, J. Market, E. Petre, D. Spain, and T. Odumosu, 2010, Petrophysical Evaluation for Enhancing Hydraulic Stimulation in Horizontal Shale Gas Wells: SPE 132990-MS, 21 p.

Curtis, M.E., R.J. Ambrose, C.H. Sondergeld, and C.S. Rai, 2011, Transmission and scanning electron microscopy investigation of pore connectivity of gas shales on the nanoscale: SPE144391-MS, 10 p.

Curtis, M.E., R.J. Ambrose, C.H. Sondergeld, and C.S. Rai, 2011, Investigating the microstructure of gas shales by FIB/SEM tomography and STEM imaging: University of Oklahoma, 28 p.

Fryman, M., 2010, Determinations of the dynamic elastic constants of a transverse isotropic rock based on borehole dipole sonic anisotropy in deviated wells: Paper IBP2304_10, Rio Oil & Gas Expo Conference, Rio de Janeiro, Brazil, 13–16 September.

Herron, M.M., J.A. Grau, S.L. Herron, R.L. Kleinberg, M. Machlus, S.L. Reeder, B. Vissapragada, A.K. Burnham, R.L. Day, and P. Allix, 2011, Total organic carbon and formation evaluation with wireline logs in the Green River oil shale: SPE 147184, 19 p.

Higgins, S., S. Goodwin, A. Donald, T. Bratton, and G. Tracy, 2008, Anisotropic Stress Models Improve Completion Design in the Baxter Shale: SPE 115736, 10 p.

Hornby, B.E., J.M. Howie, and D.W. Ince, 2003, Anisotropy Correction for Deviated-Well Sonic Logs: Application to Seismic Well Tie: Geophysics, v. 68/2, p. 464-471.

Market, J., J. Quirein, J. Pitcher, D. Hinz, D. Buller, C. Al-Dammad, D. Spain, and T. Odumosu, 2010, Logging-While-Drilling in unconventional shales: SPE 133685, 18 p.

Parker, M., D. Buller, E. Petre, and D. Dreher, 2009, Haynesville shale–petrophysical evaluation: SPE 122937, 11 p.

Passey, Q. R., S. Creaney, J.B. Kulla, F.J. Moretti, and J.D. Stroud, 1990, A Practical Model for Organic Richness from Porosity and Resistivity Logs: AAPG Bulletin, v. 74/12, p. 1777-1794.

Quirein, J., J. Witkowsky, J. Truax, J. Galford, S. Spain, and T. Odumosu, 2010, Integrating core data and wireline geochemical data for formation evaluation and characterization of shale gas reservoirs: SPE 134559, 18 p

Quirein, J., J. Galford, J. Witkowsky, D. Buller, and J. Truax, 2012, Review and comparison of three different gas shale interpretation approaches: Presented at the 53rd Annual SPWLA Logging Symposium, Cartagena, Columbia.

Ramirez, T.R., J.D. Klein, R.J.M. Bonnie, and J.J. Howard, 2011, Comparative study of formation evaluation methods for unconventional shale-gas reservoirs: application to the Haynesville Shale (Texas): SPE 144062, 31 p

Rickman, R., M. Mullen, E. Petre, B. Grieser, and D. Kundert, 2008, A practical use of shale petrophysics for stimulation design optimization: SPE 115258, 11 p

Schoenberg, M., F. Muir, and C. Sayers, 1996, Introducing Annie: A Simple Three-Parameter Anisotropic Velocity Model for Shales: Journal of Seismic Exploration, v. 5, p. 35-49.

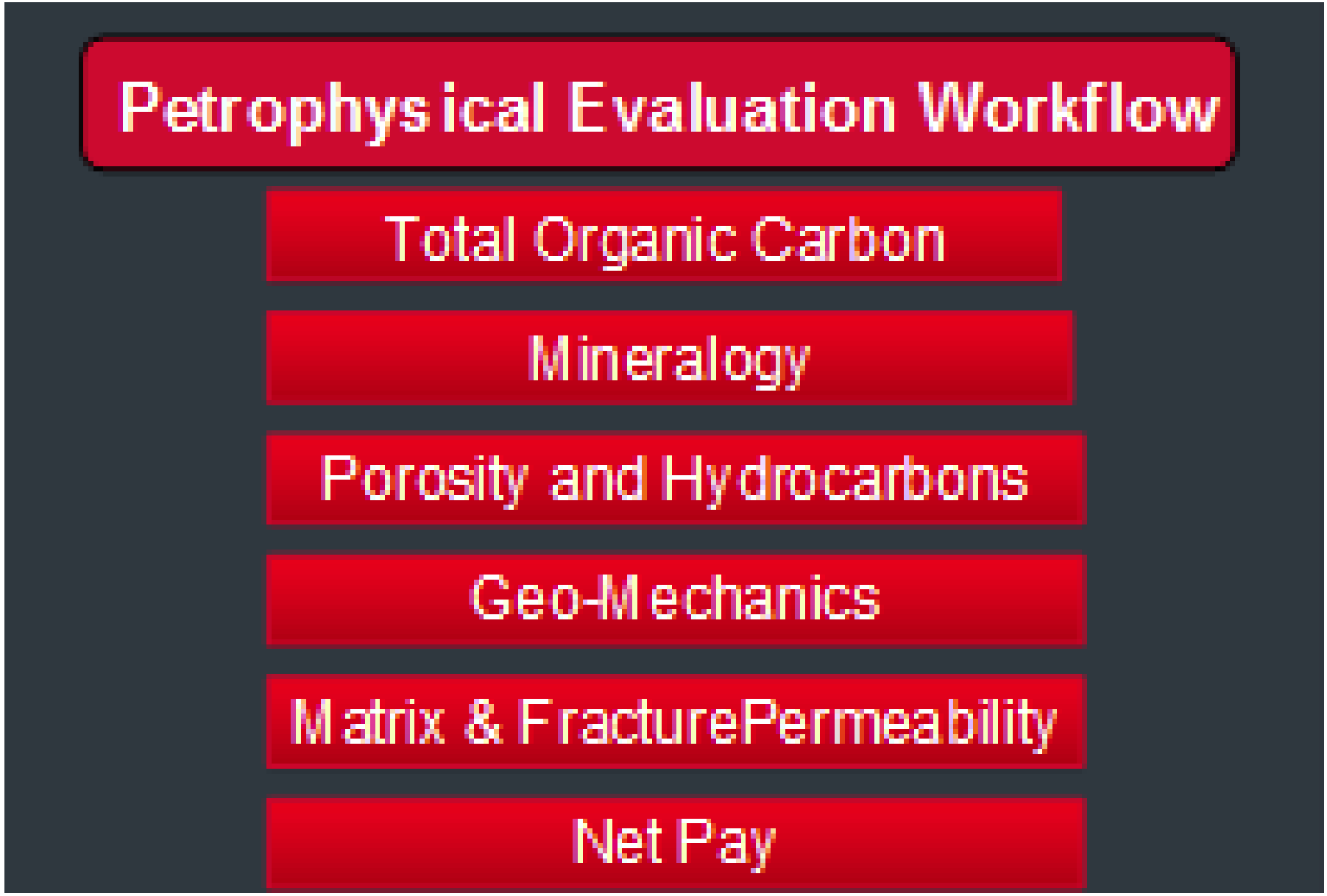

Figure 1. Shale reservoir petrophysical evaluation workflow.

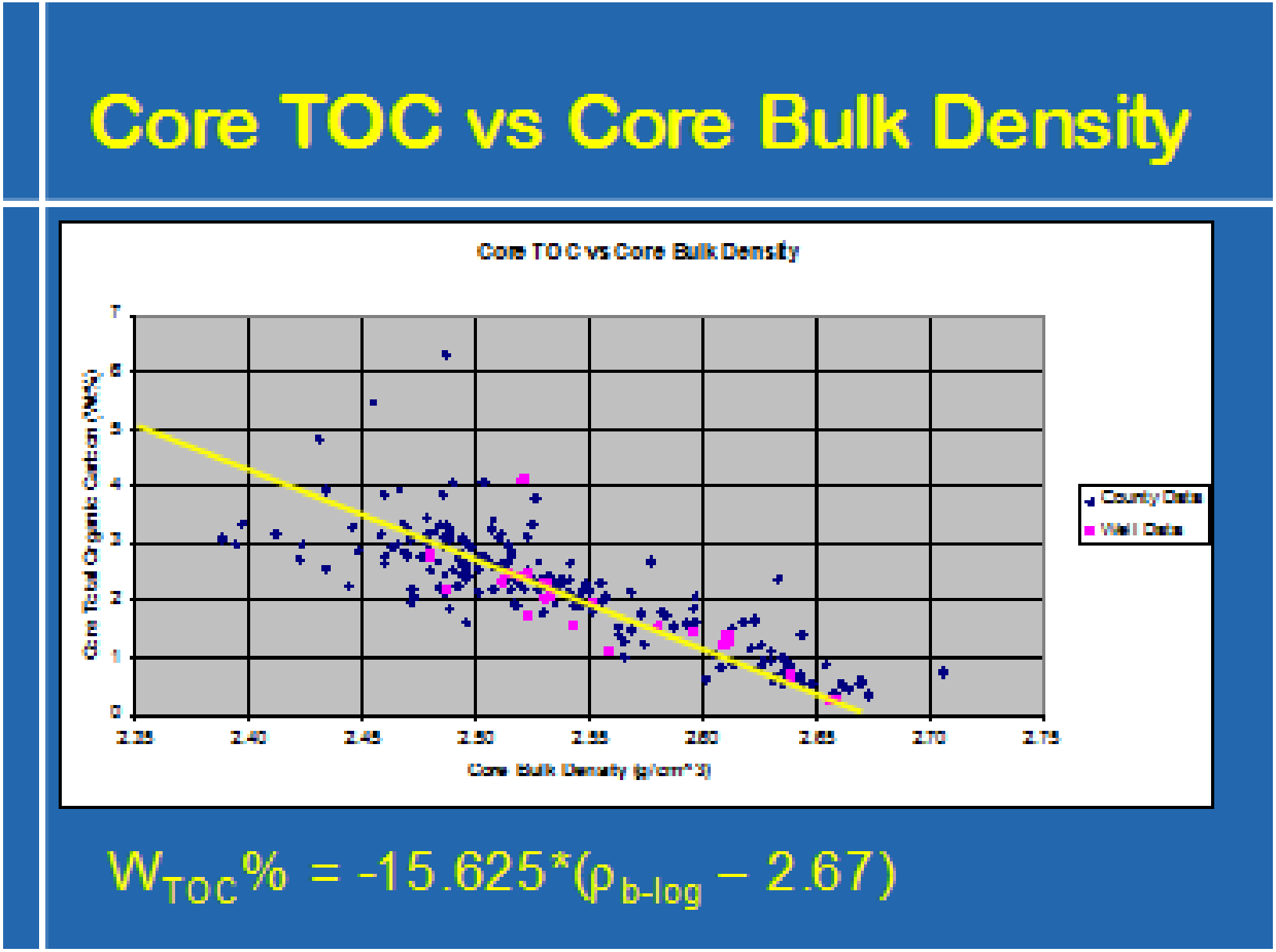

Figure 2. Predicting wt% TOC directly from core bulk density (from Quirein et al. 2010).

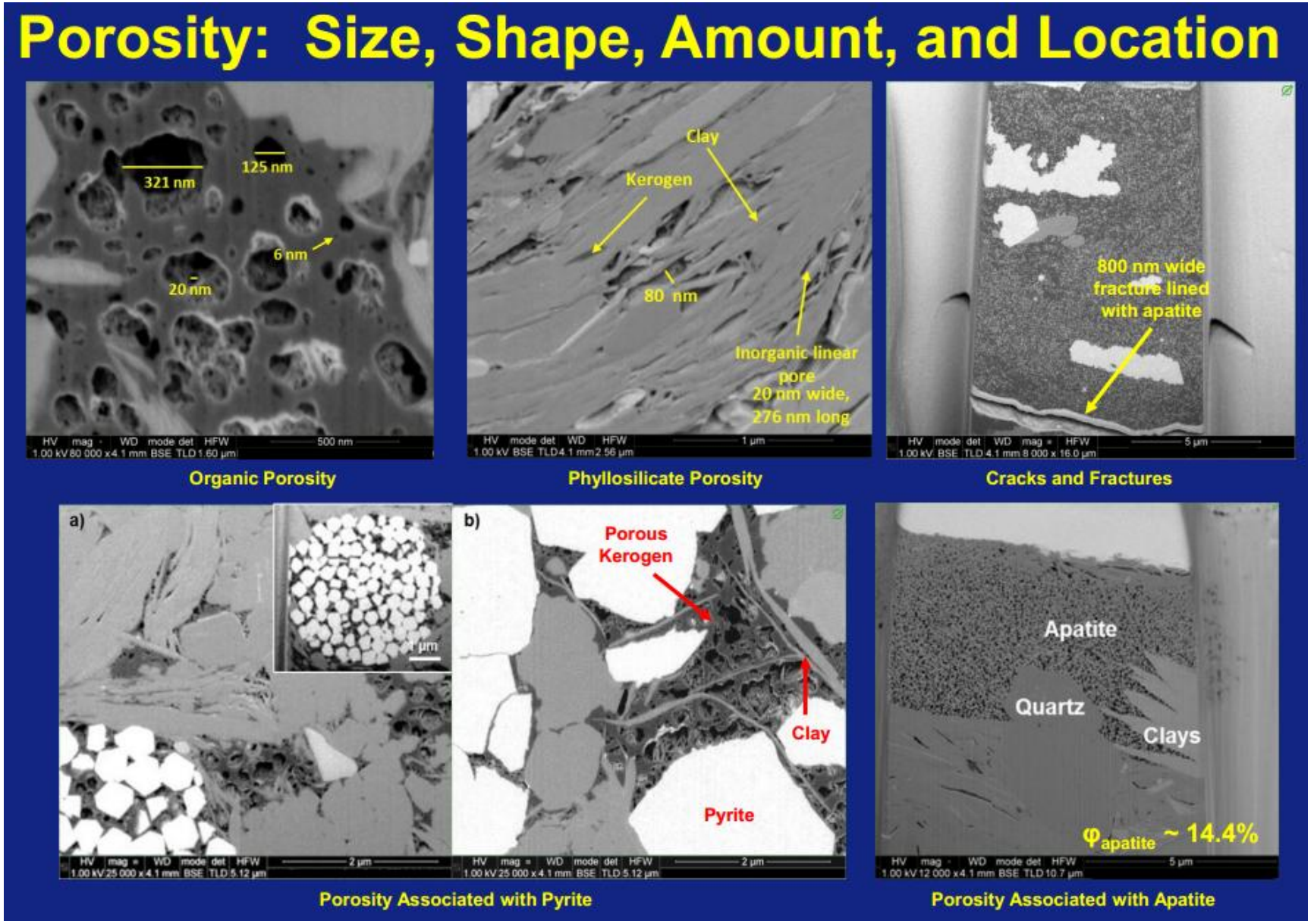

Figure 3. Different shale porosity types as imaged by Curtis et al. 2011.

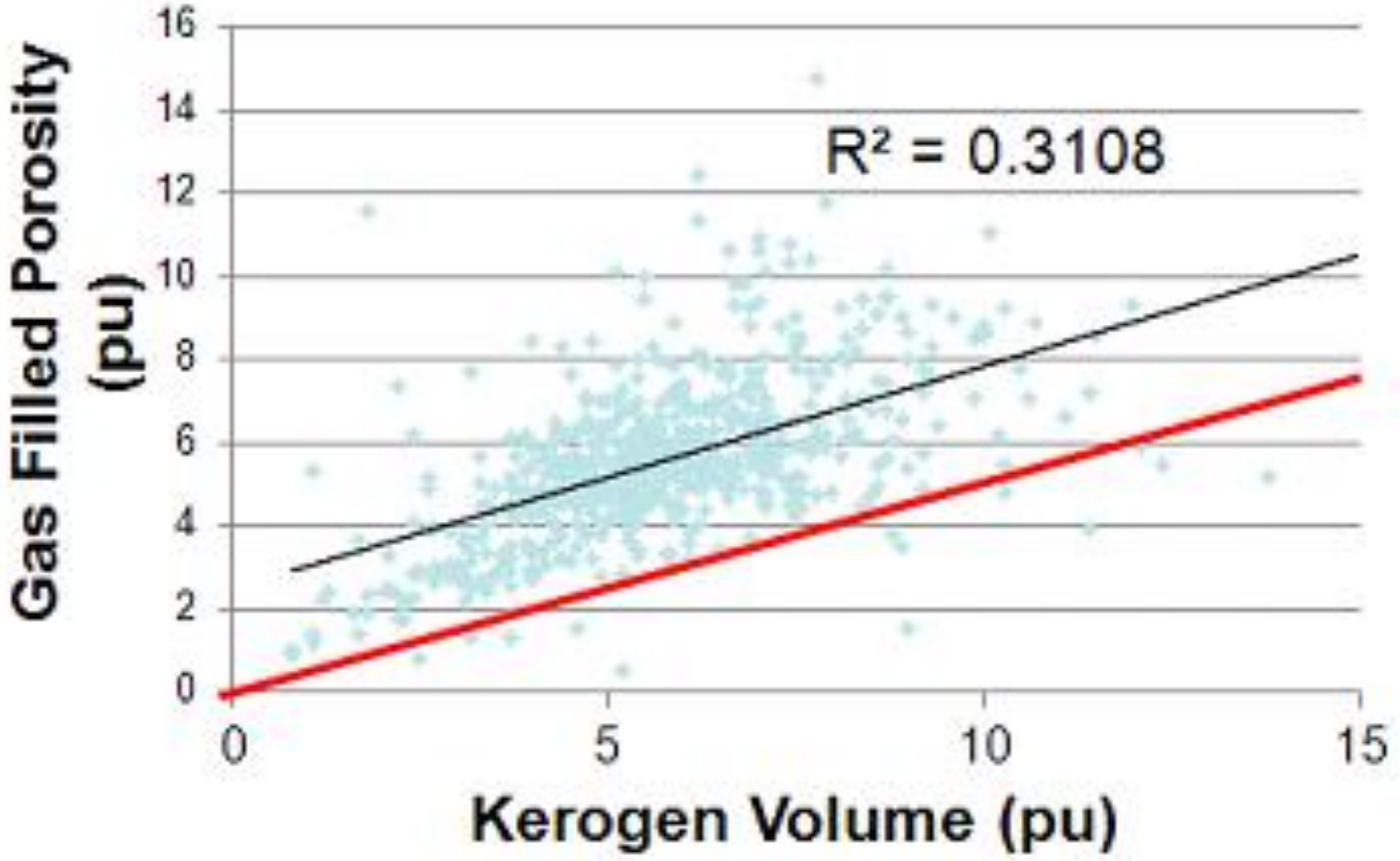

Figure 4. Weak correlation between gas-filled porosity and kerogen. The red line is a mathematical representation of a kerogen porosity of 33 pu. The fact that all the data lies above the line suggest a dual- porosity system.

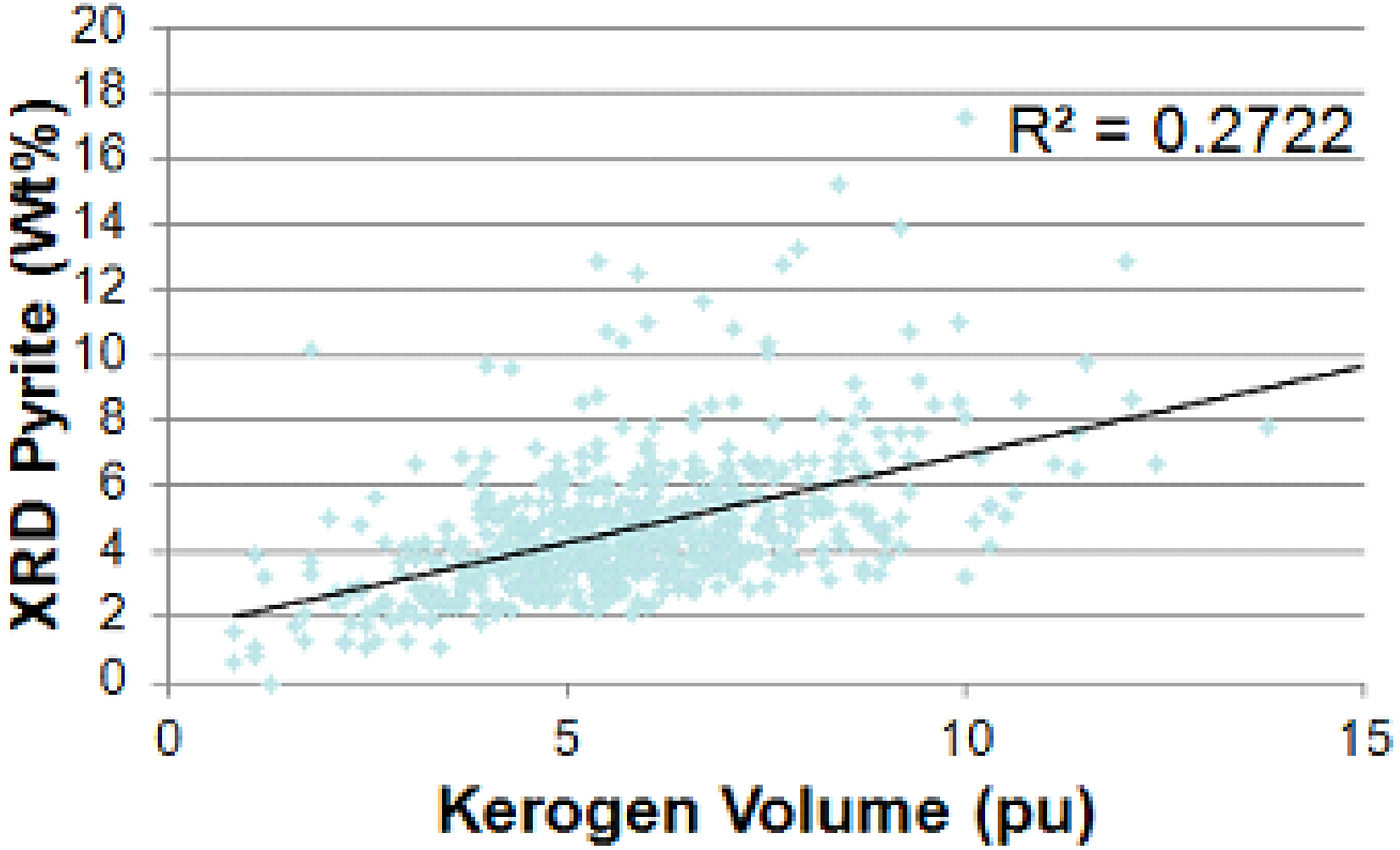

Figure 5. Weak correlation between XRD pyrite and kerogen.

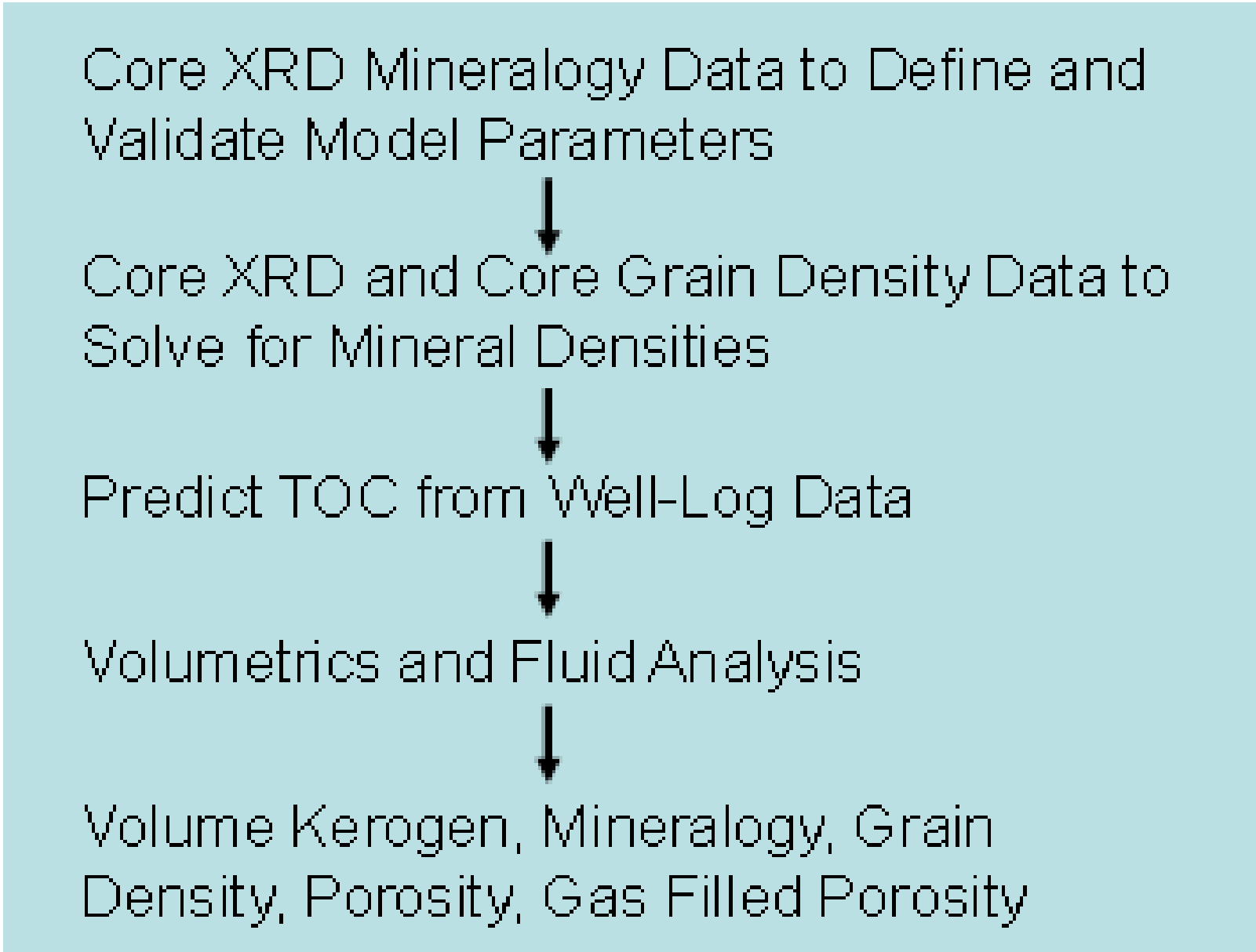

Figure 6. Summary of the workflow proposed by Quirein et al. (2010).

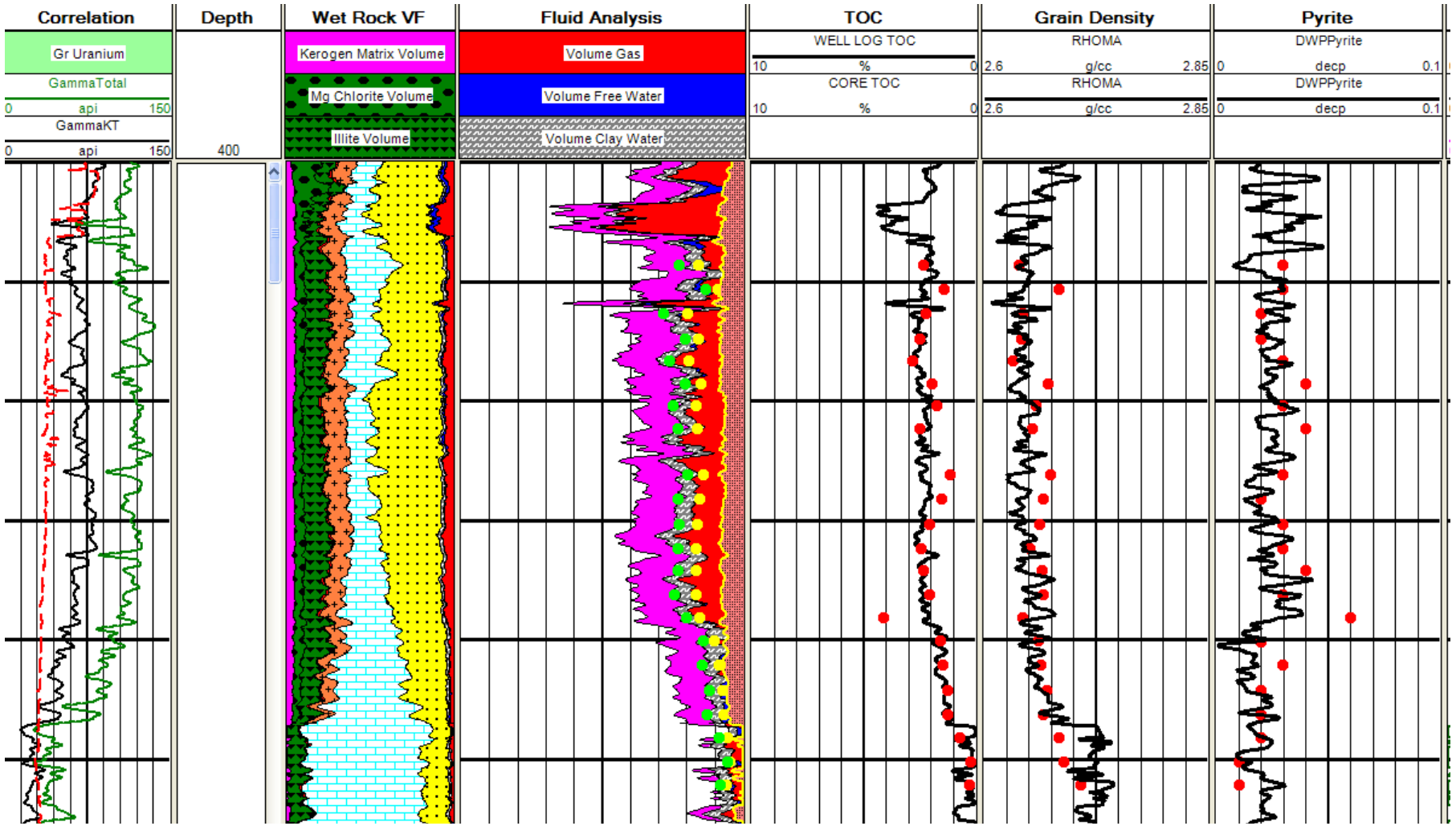

Figure 7. Interpretation results for a representative Haynesville well from Quirein et al. 2012.

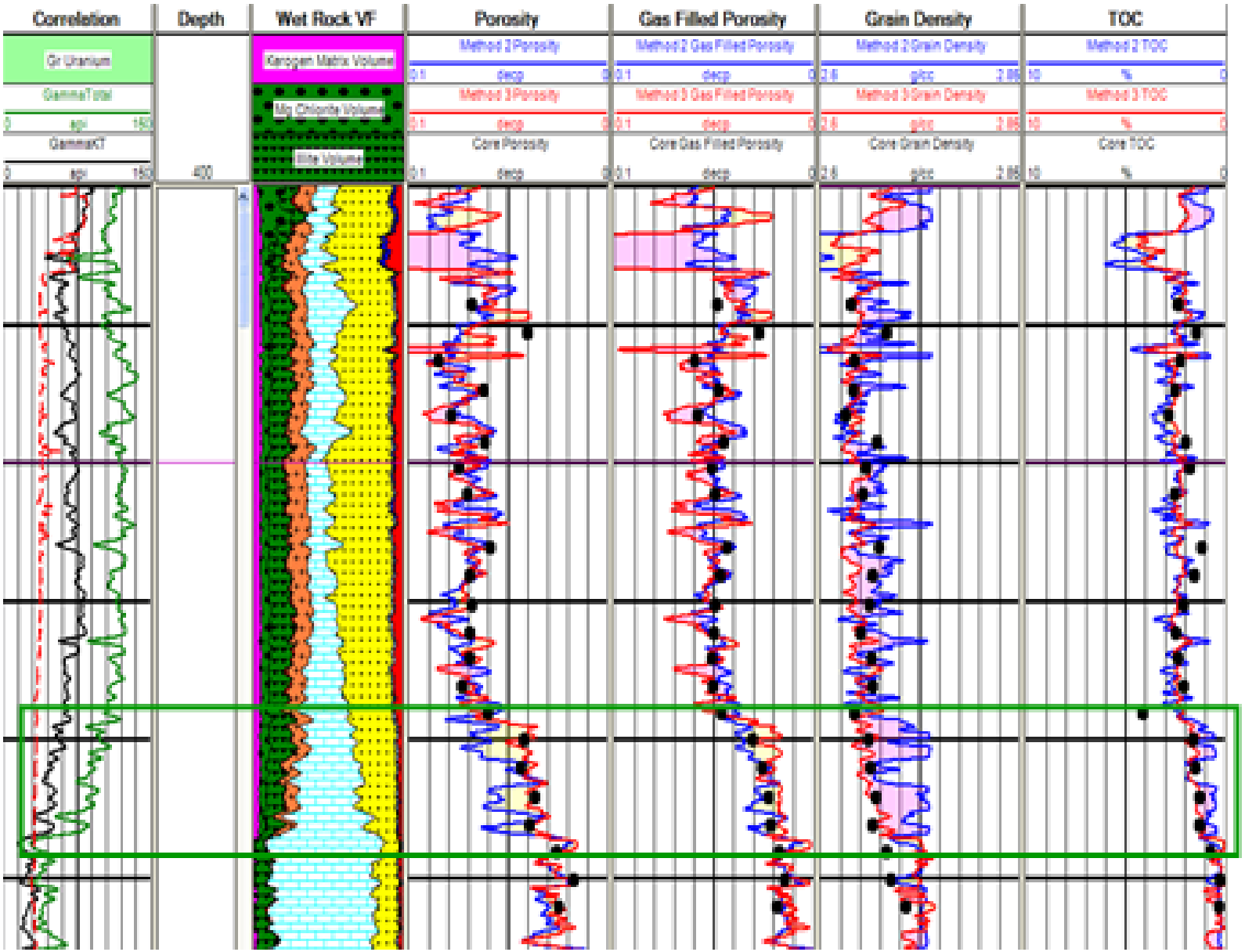

Figure 8. Comparison of two approaches with core data from Quirein et al. 2012.

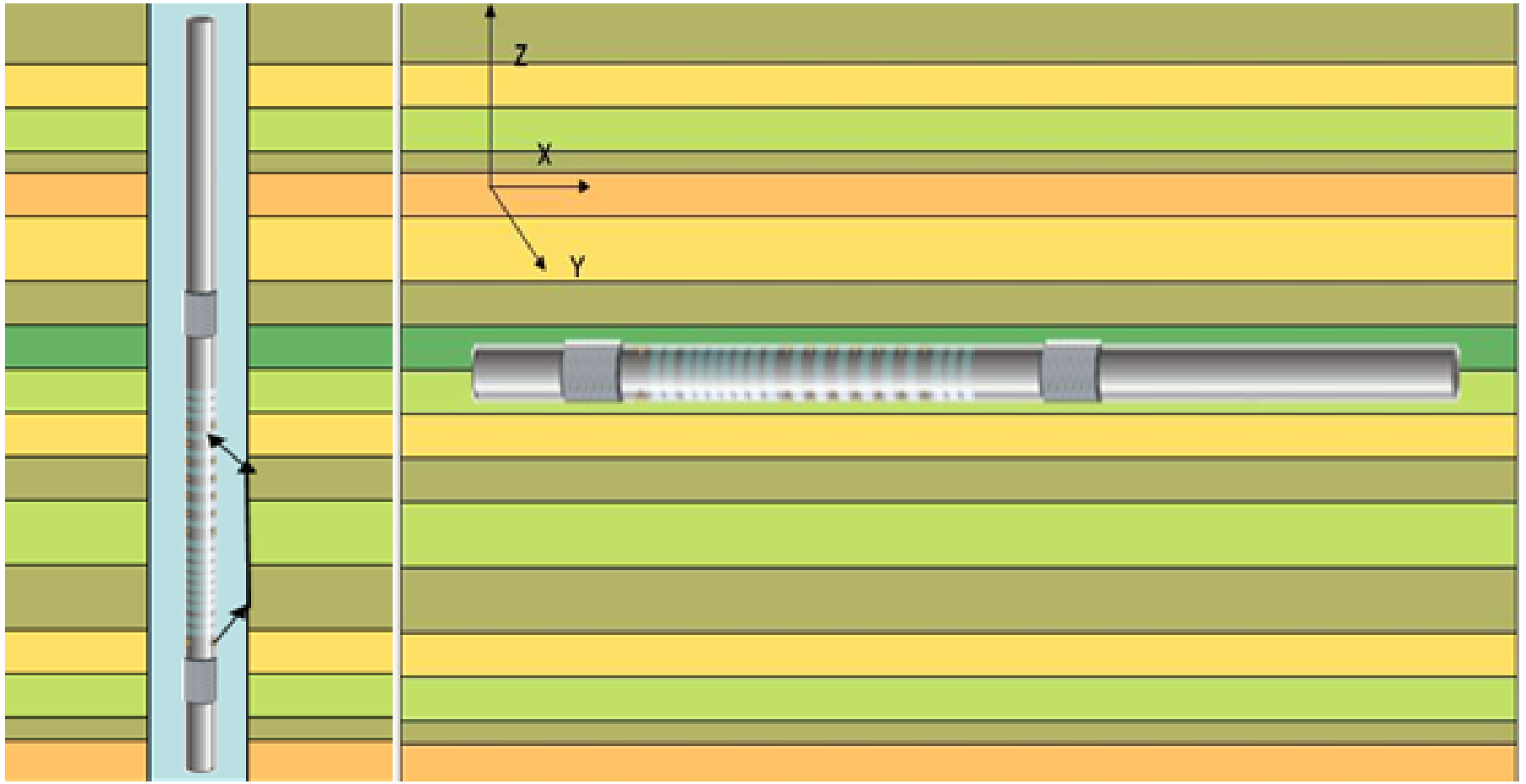

Figure 9. Sonic tool in fine-layered media; Left (a) vertical; Right (b) horizontal.

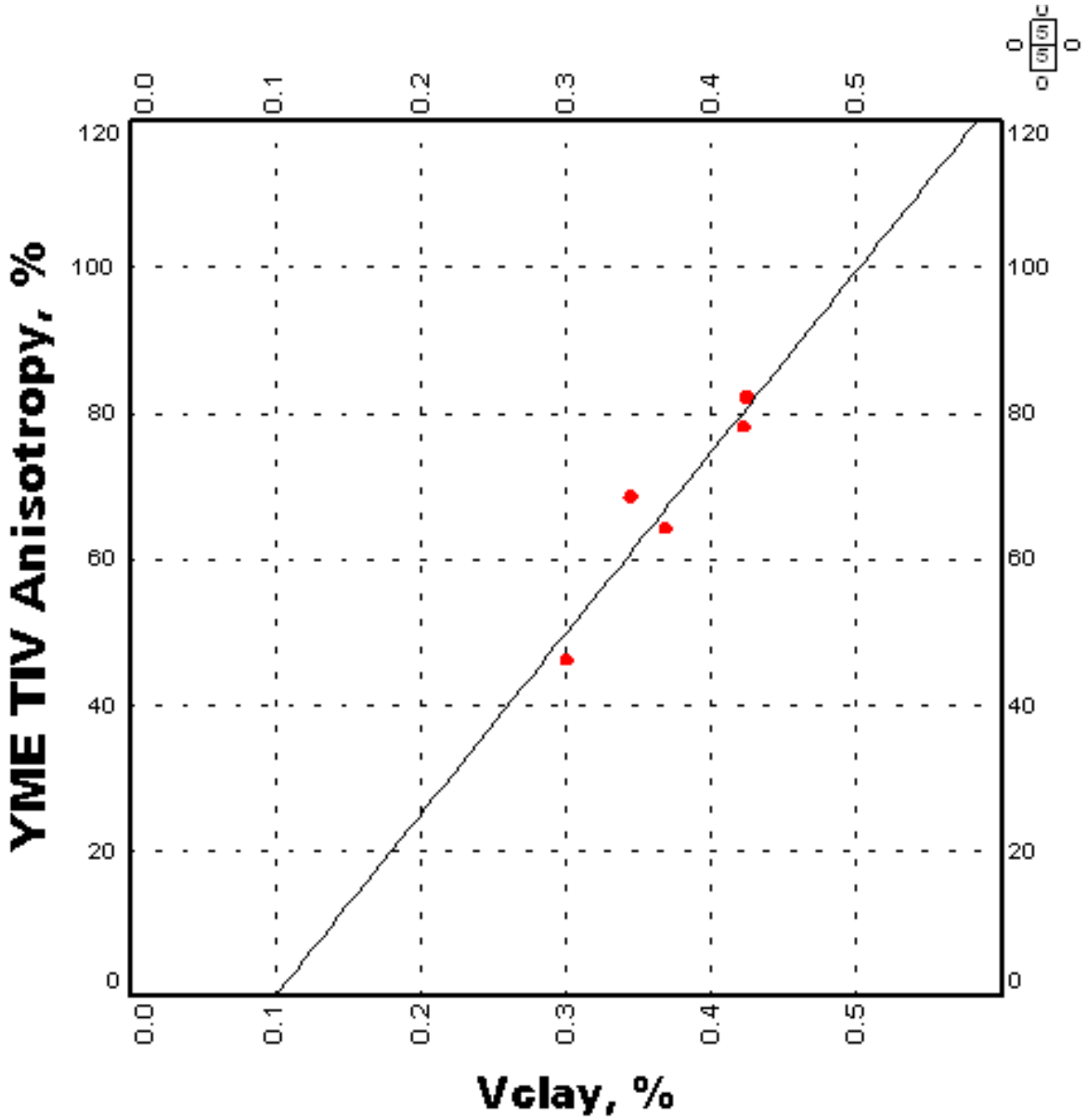

Figure 10. Youngs Modulus TIV anisotropy vs. clay volume.

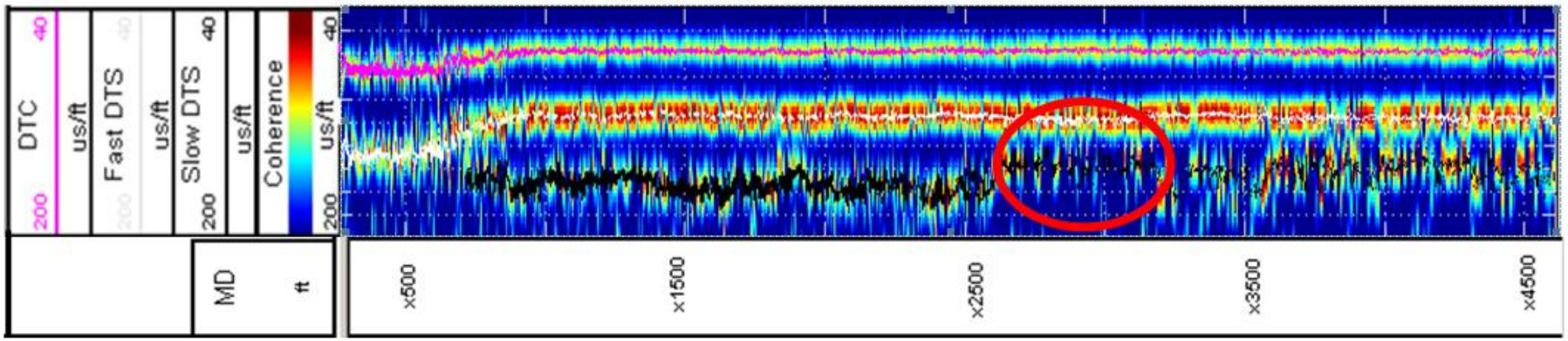

Figure 11. Sonic log example from the Haynesville shale. This example shows both the landing (<x700 ft) and horizontal portion of the well (>x700 ft), which was steered to remain within one zone. The fast shear (white) reflects little change in the y. axis velocity, whereas the slow shear (black) responds to the changes in the z. axis and shows considerable variation. The zone circled in red is the most brittle in the z. direction, whereas the brittleness in the y. direction is nearly uniform (because we are drilling within the same layer), so this is the ideal production zone.

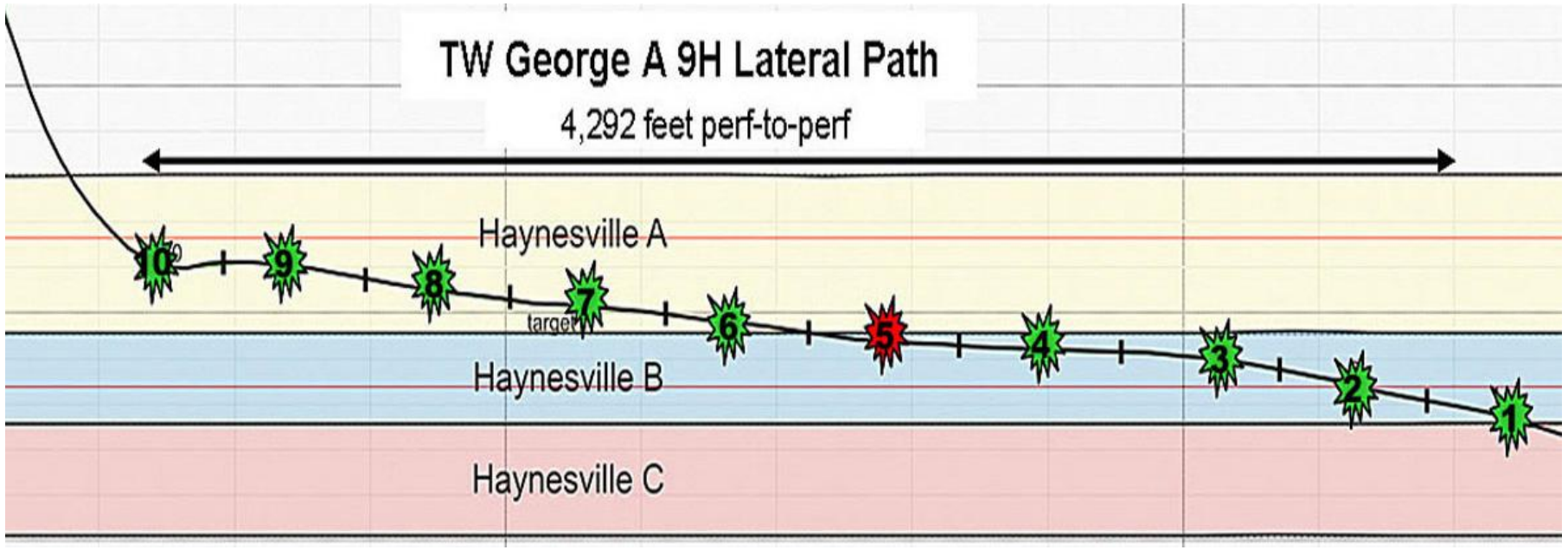

Figure 12. BP, T.W. George A9H correlated 4,300 ft lateral path within the Haynesville Shale. Green-numbered frac stages were considered successful with proppant placed. Stage 5 screened out with no placed proppant.

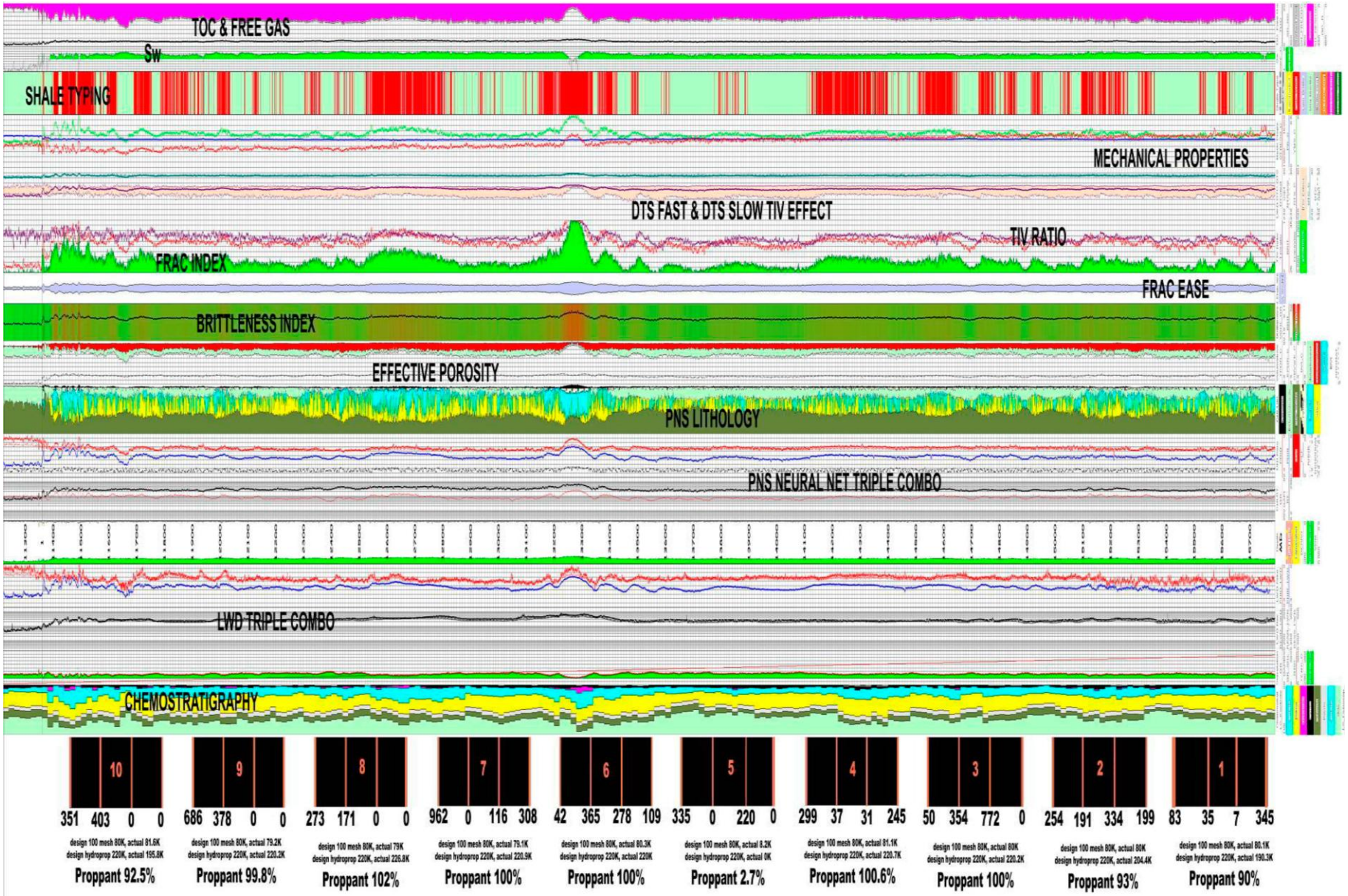

Figure 13. BP, T.W. George A9H Horizontal Shale Evaluation, L. R: Frac Stage perfs, production, & placed proppant, LIBS Chemostratigraphy, LWD Triple Combo, PNS Neural Net Triple Combo & Spectral Yield Lithology, effective porosity, brittleness index, frac index, LWD TIV ratio, DTS slow & DTS fast TIV anisotropy effect, mechanical properties, shale classification, Sw, TOC, and free gas.

Criteria	Porosity (p.u.)	Gas-Filled Por. (p.u.)	TOC (Wt %)	Grain Density (g/cc)
Correlation Coeff.	0.89	0.91	0.71	0.67
RMSE	0.89	0.56	0.62	0.014
Average Error	0.16	-0.04	0.13	-0.004

Table 1. Summary prediction statistics comparing the interpretation to core data.